Nucleic Acids Research, 2001, Vol. 29, No. 3 753–758

Pseudoknots in prion protein mRNAs confirmed by comparative sequence analysis and pattern searching

Isabelle Barrette, Guylaine Poisson, Patrick Gendron and François Major*

Département d'Informatique et de Recherche Opérationnelle, Université de Montréal, CP 6128, Succ. Centre-Ville, Montréal, Québec H3C 3J7, Canada

Received September 12, 2000; Revised November 22, 2000; Accepted December 1, 2000

ABSTRACT

The human prion gene contains five copies of a 24 nt repeat that is highly conserved among species. An analysis of folding free energies of the human prion mRNA, in particular in the repeat region, suggested biased codon selection and the presence of RNA patterns. In particular, pseudoknots, similar to the one predicted by Wills in the human prion mRNA, were identified in the repeat region of all available prion mRNAs available in GenBank, but not those of birds and the red slider turtle. An alignment of these mRNAs, which share low sequence homology, shows several co-variations that maintain the pseudoknot pattern. The presence of pseudoknots in yeast Sup35p and Rnq1 suggests acquisition in the prokaryotic era. Computer generated three-dimensional structures of the human prion pseudoknot highlight protein and RNA interaction domains, which suggest a possible effect in prion protein translation. The role of pseudoknots in prion diseases is discussed as individuals with extra copies of the 24 nt repeat develop the familial form of Creutzfeldt–Jakob disease.

INTRODUCTION

Approximately 15% of all documented human Creutzfeldt–Jakob disease (CJD) cases are due to inherited mutations. In one particular case additional copies of an octapeptide are inserted in the unstructured N-terminal domain of the prion protein. In fact, four to nine extra copies of a 24 nt repeat in the prion protein (PrP^c) gene are implicated in development of the disease (1–4). Normally the human prion gene contains five copies of this repeat, which is highly conserved among species in prion genes (5) and has even been found in the yeast prion protein Sup35p (6). The repeats might have appeared through unequal crossover events (4) and vary in number among species and individuals. Recently it was demonstrated that cloning in mice of a mouse homolog of the human prion gene containing four extra repeats caused the occurrence of a prion disease whose symptoms resembled those of human familial CJD (7). Moreover, it was later shown that expression of PrP^c containing 14 copies of the repeat in mice resulted in apoptosis of cerebellar granule cells (8). However, the exact function of these repeats has remained elusive. The oligopeptides resulting from the repeats have been shown to bind copper and it was suggested that PrP^c diseases could be due to defective copper metabolism (9). Recently, however, the prion protein's role in copper metabolism was challenged by the finding that over-expression of PrP^c did not alter copper levels in mice (10).

Thermodynamic analyses of the 24 nt repeat region suggest the presence of several hairpin loop structures (11,12), but, more interestingly, Wills proposed the presence of a RNA pseudoknot (Fig. 1A; 13). Pseudoknots are known to interfere with translation speed and to cause frameshifting (14). However, it is now known that frameshifting does not occur in prion diseases, but rather that all strains of the scrapie form of the prion protein (PrP^{Sc}) are composed of the same polypeptide sequence (15).

In an attempt to identify functional RNAs in prion genes we performed an extensive analysis of the folding free energies of the prion mRNA. These analyses are based on the work by Le and Maizel (16) and Seffens and Digby (17), who reported that mRNAs contain fragments of greater negative folding energies than their shuffled or codon choice randomized counterparts. Forsdyke, who inspired us, performed the same type of studies on DNA and cDNA and observed similar results (18). In some cases the codon choice in mRNA and DNA is biased to conserve functional elements, which may participate in regulatory processes (14,19,20).

We developed a computer program, a RNA Structural Pattern Finder, which was used to indicate the presence of possible codon choice biased regions in the human prion mRNA, in particular in the 24 nt repeat region. More importantly, using the computer program RNAMOT (21) a prion pseudoknot descriptor was developed, which allowed us to find similar pseudoknots in the repeat region of all prion mRNA sequences currently contained in GenBank, but not those of birds and the red slider turtle. The prion mRNA sequences are not homologous in the repeat region, as has been demonstrated using the BLAST sequence homology program (22). We present an alignment of the mRNA sequences in the repeat region which shows several co-variations to maintain the pseudoknot pattern. The presence of pseudoknots in yeast Sup35p and Rnq1 and the fact that Rnq1 does not possess the 24 nt repeat suggest acquisition of pseudoknots in the

*To whom correspondence should be addressed at present address: Isis Pharmaceuticals Inc., 2292 Faraday Avenue, Carlsbad, CA 92008, USA. Tel: +1 760 603 2677; Fax: +1 760 431 2768; Email: major@iro.umontreal.ca

The authors wish it to be known that, in their opinion, the first two authors should be regarded as joint First Authors

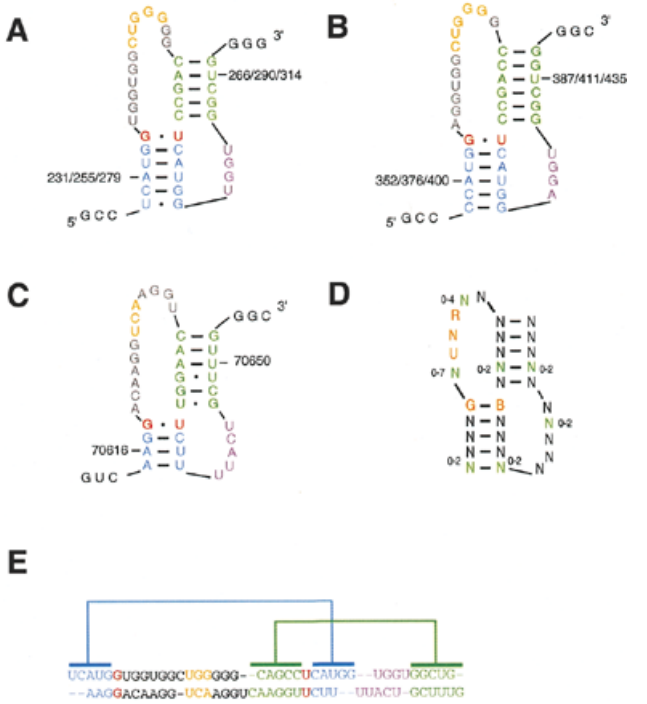

Figure 1. Prion pseudoknot secondary structures. The nucleotides are colored as follows: the G-U wobble base pair is in red, the major loop is in gray, the minor loop is in violet and the stems are in cyan and green. (**A**) The pseudoknot described by Wills (13) in humans. The CUGGG motif is in yellow. (**B**) The pseudoknot found in cattle. The CUGGG motif is in yellow. (**C**) The pseudoknot found in yeast Rnq1. The UCA motif is in yellow. (**D**) A generalization of the prion pseudoknot motif, as used in the RNAMOT program. N, any nucleotide; R, purine; B, C, G and U. The green nucleotides indicate flexible regions that could contain the number of nucleotides indicated by its corresponding range. (**E**) The alignment of the distant pseudoknots shown in (A) and (C).

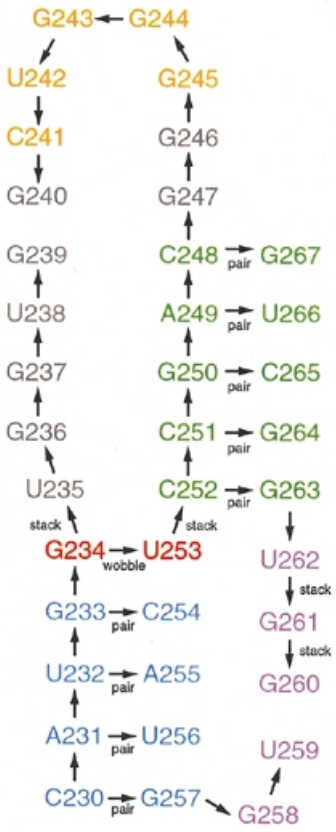

Figure 2. MC-SYM script for the human prion pseudoknot. The arrows represent nucleotide relations. The arrows start from the reference to the placed nucleotide. For instance, C230 is the global reference nucleotide. It was used to stack A231 and to pair G257, A231 was used to pair U256, and so on. Unlabeled arrows indicate the 'connect' relation, which includes 'stack' and 'bulged out' relations, except in stems, where they indicate helical stacking. The label 'pair' indicates that all hydrogen bonding patterns were tentatively assigned for the given pair of nucleotides. The nucleotides are colored following the rules of Figure 1.

prokaryotic era. Three-dimensional (3-D) structures of the human prion pseudoknot were built using the molecular modeling package MC-SYM (23). Some structures highlight the UNR (U-turn) motif in the major loop of the pseudoknot, which exposes to the solvent chemical groups that usually interact with proteins and/or other RNAs. Finally, a possible role in the familial form of CJD is discussed.

MATERIALS AND METHODS

Analysis of the folding free energies of human PrP^c mRNA

The total folding free energy (E) of a RNA sequence results from base order and composition (18) and represents the minimum of its free energy profiles (16). One way of measuring E is by determining base pairing and stacking energies from its most stable predicted secondary structure. For instance, we compute E using the dynamic programming algorithm and thermodynamic parameters implemented by Rivas and Eddy (24). To compute the base order-dependent E value of a sequence we compare E with E_r, the average energy of sequences obtained from randomly permuting its base order. E_r reflects the base composition-dependent energies. The base order-dependent energies are given by the difference between E and E_r, $\Delta E = E - E_r$. Negative values of ΔE indicate that the choice of codons in a particular region could be biased in order to accommodate functional elements (18).

We developed a Structural Pattern Finder (SPF) computer program for detecting the regions of a RNA sequence where E significantly deviates from E_r. The RNA sequence is divided into n windows of m nt, which overlap the preceding window by l nt. Each window is folded and its E value measured. Then, all of the windows are shuffled x times and folded again. In this work the 2415 nt human prion mRNA (GenBank accession no. NM_000311) was divided into 45 windows of 200 nt overlapping the preceding ones by 150 nt and each window was shuffled 500 times. Statistical significance was tested for biases observed in the calculated E values between the native human prion mRNA and the 500 randomized sequences.

Pseudoknot motif search

RNAMOT (21) was used to search for pseudoknots in 87 mRNA sequences taken from GenBank. The RNAMOT descriptor was developed from the secondary structure of the

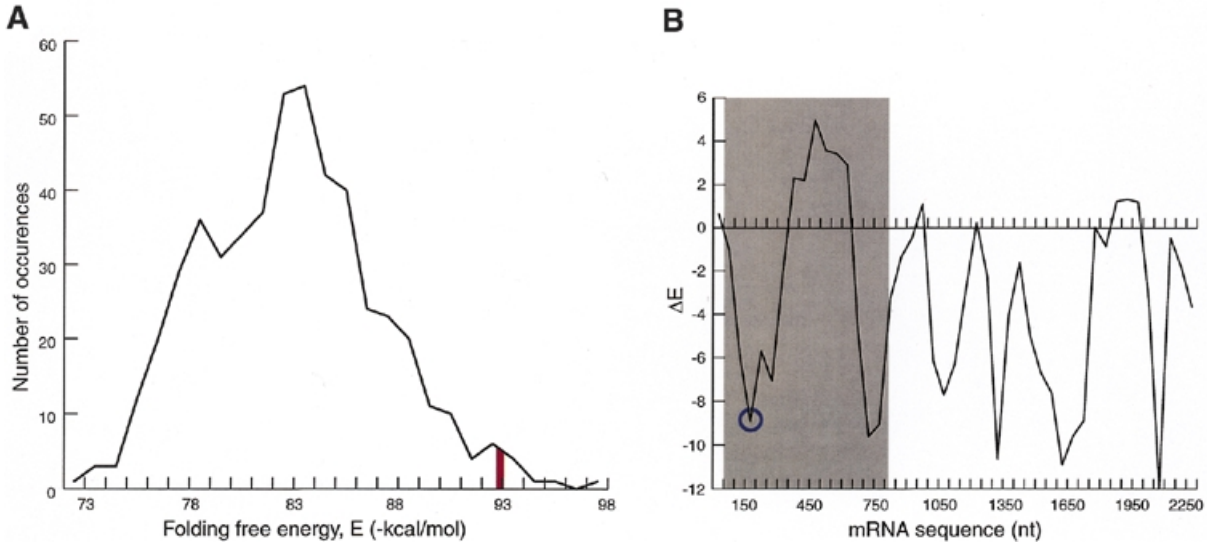

Figure 3. Folding free energy distribution of the human prion gene. (**A**) Distribution of the *E* values of the shuffled sequences from the fourth 200 nt window encompassing nucleotides 150–350. The red bold line represents the *E* value of the fourth window in the native sequence. (**B**) Δ*E* of the 45 windows. The Δ*E* values of windows in the coding sequence, nucleotides 50–811, are shown in the gray area. The Δ*E* peak of the fourth window is circled in blue.

pseudoknot predicted by Wills in human prion mRNA (13). The descriptor was generalized (Fig. 1D) to accommodate sequence and structure variations in the other prion mRNAs, such as those shown in Figure 1B and C. Four to six base pairs were allowed in stems I and II. The UNR motif in loop I is a key element since it might be implicated in RNA–protein (12) and RNA–RNA interactions (25). In loop I up to 7 nt were allowed 5′ of the UNR motif and 1–5 nt were allowed 3′ of it. Four to six nucleotides were allowed in loop II, without any sequence restraints. The length parameters for the stem–loops were fixed in order to optimize similarity with the human prion pseudoknot described by Wills, as well as to respect the thermodynamics of RNAs. The last base pair in stem I was restricted to G-B, as it has been shown to be important in RNA–protein interactions (26).

RNAMOT was run on a dual Intel 600 MHz Pentium III processor PC with 1 GB of RAM to search for pseudoknots in the sequences with the following GenBank accession nos: AF003087, AF009181, AF015603, AF090852, AF113937, AF113938, AF113939, AF113941, AF113942, AF113943, AF113944, AF113945, AF117309, AF117310, AF117311, AF117312, AF117313, AF117314, AF117315, AF117316, AF117317, AF117318, AF117319, AF117320, AF117321, AF117322, AF117323, AF117324, AF117325, AF117326, AF117327, AF117328, AF117329, AF157954, AF157955, AF157956, AF157957, AF157958, AF157959, AF157960, AJ223072, AJ245488, D50093, K02234, L07623, M13685, M21129, M33958, M61145, M95404, NC_001135, NM_000311, U08291, U08292, U08293, U08294, U08295, U08296, U08297, U08298, U08299, U08300, U08301, U08302, U08303, U08304, U08305, U08306, U08307, U08308, U08309, U08310, U08311, U08312, U08952, U21210, U28334, U75382, U75383, U75384, U75385, U75386, U75387, U75388, U75389, X74759, Y09760, Y09761.

3-D modeling of the PrP^c mRNA pseudoknot

The MC-SYM molecular modeling computer program (23) was used to generate 3-D structures of the human prion pseudoknot. An input script describing the human prion pseudoknot secondary structure predicted by Wills (13) was defined (see Fig. 2). The standard A-RNA conformation found in double helical regions was assumed for the two stems. A wobble hydrogen bonding pattern was assigned to the G-U base pair at the end of the first stem. The nucleotides in the minor loop region were assigned C3′-*endo* sugar pucker modes combined with *anti* base orientations, as defined by the torsion around the glycosyl bond. The nucleotides in the major loop were allowed to adopt any conformation. The MC-SYM program was run on a dual Intel 600 MHz Pentium III processor PC with 1 GB of RAM. The MC-SYM program is available at www-lbit.iro.umontreal.ca/mcsym/.

The potential energies of the generated structures were minimized using the program CHARMm (27) and the CHARMm force field parameters 1997 (28). The minimization was performed using a distance-dependent constant dielectric ($\varepsilon = 4r$). The obtained structures were then used to calculate the electrostatic solvation free energy using the program UHBD (29) with a grid of 100^3 points separated by 0.8 Å. The Poisson–Boltzmann linear equation was applied with a bulk salt concentration of 400 mM. The sums of the potential energies obtained in CHARMm and the electrostatic solvation free energies calculated in UHBD were used to compare the structures. CHARMm was run on a dual Intel 600 MHz Pentium III processor PC with 1 GB of RAM.

RESULTS

Folding free energies

The randomized human prion mRNA *E* values are normally distributed, as shown in Figure 3A. The fourth window of the

Figure 4. Alignment of 78 mRNA sequences according to the pseudoknot structure. The nucleotides are colored following the rules of Figure 1.

native sequence, containing the repeat region, has one of the lowest energy values obtained, E = –92.7 kcal/mol. E_r of the shuffled sequences for the fourth window, –83.8 ± 0.4 kcal/mol, is approximately two standard deviations different from the native sequence, suggesting a possible evolutionary biased codon selection. The error margin from the 500 shuffled sequences was at a confidence level of 95%. Several other regions were identified as possibly being under evolutionary biased codon selection (Fig. 3B), but the fourth window has one of the largest ΔE values obtained.

Motif search

Pseudoknots were located in all 76 mammalian prion genes contained in GenBank, as well as in the yeast prion genes Sup35p and the recently discovered Rnq1 (30). The only species in which no pseudoknots were found are the nine available birds and the red slider turtle (31), which possess genes significantly different from the others (5,31). The secondary structures of human, bovine and yeast pseudoknots are shown in Figure 1A–C. The rate of false positives was computed by searching for prion pseudoknots in 1000 randomly generated sequences of 120 nt. Our descriptor matched 90 random sequences, which gives a false positive rate of ~0.09.

An alignment of the 78 mRNA sequences in the pseudoknot region is shown in Figure 4. The pseudoknots were classified into nine groups based on sequence similarity. Using BLAST (22), the human pseudoknot sequence did not match the two yeast pseudoknot sequences, although there was a striking similarity in pseudoknot structure. Considering the nine groups as nine independent evolutionary events, one could estimate the likelihood of finding by chance the prion pseudoknot in these 78 genes, using the RNAMOT rate of false positives, to be $<1/10^9$. However, since it is unusual to consider the 76 mammalian sequences as arising from independent events, we considered two groups only, which gave us a likelihood of finding by chance the prion pseudoknot in mammals and yeast of $0.09^2 = 0.008$.

3-D modeling of the prion pseudoknot

Using the input script shown in Figure 2, the molecular modeling computer program MC-SYM (23) generated multiple structures of the human pseudoknot. After visual inspection and energy minimization with CHARMm (27,28) and UHBD (29) a subset of different structures, shown superimposed in Figure 5, was selected (available at www-lbit.iro.umontreal.ca/en/archives). In some of these structures a hydrogen bond forms between the uridine of the UNR motif and the phosphate of the nucleotide following the R. These structures exemplify how the UNR motif and some stacked nucleotides, as well as

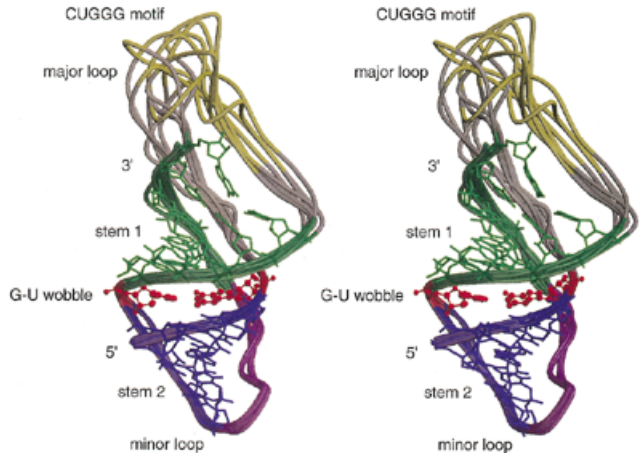

Figure 5. Stereoview of a superimposition of several different pseudoknot 3-D structures. The ribbon joins the phosphates. The ribbon and nucleotides are colored following the rules of Figure 1.

the G-U base pair at the end of stem I, are accessible to the solvent and could interact with proteins.

DISCUSSION

The energy analysis suggests that the human prion mRNA sequence could have been biased through evolution to conserve structural elements (Fig. 3). The region containing the 24 nt repeats possesses one of the highest ΔE values obtained, thereby supporting the presence of a functional RNA pseudoknot, first proposed by Wills (13). Using RNAMOT, this pseudoknot could be located in 78 different prion sequences, including those of yeast. The presence of a pseudoknot in yeast Rnq1 and Sup35p is extremely interesting. First, note the striking similarity between the pseudoknots in yeast Rnq1 and human PrP^c (compare Fig. 1A and C). Rnq1 has a prion domain that does not contain the 24 nt repeat. This suggests that the pseudoknot in the repeat region was probably acquired from yeast. The finding of a pseudoknot in Rnq1 also supports our low likelihood of finding the pseudoknots by chance in all mRNAs. The prion domain in Rnq1 was determined in the primary mRNA sequence from mutagenesis experiments (30). The finding of pseudoknots in the coding region of all mammals is not surprising since these sequences are very similar. However, the finding of pseudoknots in the yeast genes Sup35p and Rnq1 lends support to a possible role of this RNA pseudoknot in the conformational conversion of prion proteins.

An infrequent polymorphism occurs in the 24 nt repeats (see the alignment of the 78 mRNA sequences in Fig. 4), where the G-U wobble base pair is substituted by a G-C Watson–Crick base pair and on rare occasions by a G-G base pair. In particular, G-U and G-G base pairs at the terminal position of the stem have been observed in RNA–RNA and RNA–protein interactions (26). The UNR motif found in the major loop of the prion pseudoknots can adopt the U-turn motif known to be involved in RNA loop–loop interactions (25). The UNR U-turn motif is stabilized by a hydrogen bond between the U and the phosphate of the nucleotide following the R (32; Fig. 5). This particular arrangement exposes the acceptor and donor groups of NR and the following base to the solvent, as in the anticodon loop of tRNAs (32). The structures derived from MC-Sym were obtained in the absence of a protein and reflect the fact that at this point it is very difficult to characterize a precise pseudoknot structure. The major loop is more likely to be flexible and unstructured, but the generation of stable structures that contain a structured major loop also suggests the possibility that it can fold in a precise pattern when in contact with a protein. The CUGGG motif in the human prion pseudoknot was also found in the loop of HIV TAR RNA (12), and Tat, p68 and galectin-3 have been shown to interact with human prion mRNA (33).

The prion pseudoknot could act as a site that promotes nucleation and thus too many copies of the prion pseudoknot may interfere with proper translation and production of PrP^c. A notable example is the pseudoknot involved in translation repression of the bacteriophage T4 gene 32 protein (14,34). Thanaraj and Argos noticed that α-helices were preferentially coded by mRNA regions where the rate of translation is fast and β-strands and coils were coded by regions where the rate is slow (35). In fact, a correlation exists between the use of certain codons in the mRNA and the topological features of the resulting protein (35). This observation is interesting in the light of the conformational change occurring in PrP^c, where the mainly α-helical protein (PrP^c) attains a β-sheet-rich conformation in its infectious form (PrP^{Sc}). In this case the pseudoknot may serve as a potential therapeutic target since it has been shown that the symptoms of prion diseases may be related to the concentration of PrP^c expressed (7).

The YUNR and UNR motifs are also good targets for antisense sequences (12,25). We were interested in searching the 3′-UTR regions of the PrP^c mRNAs (results not shown) for antisense hairpins that are complementary to their associated prion pseudoknot UNR motifs in human, cattle and yeast Rnq1. Although highly speculative, the co-acquired antisense hairpins could inhibit or control the formation of pseudoknot–protein complexes.

Our observations suggest the presence of pseudoknots in the mRNAs of PrP^c genes, their actual folding and their possible involvement in and interference with PrP^c translation. Although these are yet to be demonstrated experimentally, it is tempting to suggest that these pseudoknots could be involved in the conformational changes of PrP^c to PrP^{Sc}, which occurs at the endoplasmic reticulum, where translation occurs (36). In particular, too many copies of pseudoknot–protein complexes could form and interfere with translation, leading to folding of PrP^c into its pathogenic form.

CONCLUSION

The finding of a RNA pseudoknot in 78 prion mRNA sequences, including those of yeast Sup35p and Rnq1, suggests its involvement in familial forms of CJD caused by the presence of additional 24 nt repeats. The presence of a RNA pseudoknot in primitive species such as yeast, in particular in yeast Rnq1, suggests its conservation through evolution since the prokaryotic era, an interesting phenomenon with regard to CJD and, more generally, PrP^c diseases. Using bioinformatics, a re-evaluation of the role of RNAs in familial CJD is warranted, and incisive experiments are suggested. We

are planning using our computer program SPF, combined with RNAMOT, to help us identify other RNA structures in genes implicated in other amyloid diseases, such as Alzheimer's disease.

ACKNOWLEDGEMENTS

We thank Laurent David for his help with CHARMm and UHBD and we thank Daniel Gautheret, Anthony Kusalik, Stephen Michnick and Daniel St-Arnaud, as well as the referees, for reviewing and providing useful comments and suggestions. This work was supported by a grant from the Medical Research Council of Canada (MT-14604) to F.M. G.P. holds a PhD scholarship from the Fonds pour la Formation de Chercheurs et l'Aide à la Recherche du Québec.

REFERENCES

1. Collinge,J., Beck,J., Campbell,T., Estibeiro,K. and Will,R.G. (1996) Prion protein gene analysis in new variant cases of creutzfeldt-jakob disease. *Lancet*, **348**, 56.
2. Krasemann,S., Zerr,I., Weber,T., Poser,S., Kretzschmar,H., Hunsmann,G. and Bodemer,W. (1995) Prion disease associated with a novel nine octapeptide repeat insertion in the PRNP gene. *Brain Res. Mol. Brain Res.*, **34**, 173–176.
3. Laplanche,J.L., Hachimi,K.H., Durieux,I., Thuillet,P., Defebvre,L., Delasnerie-Laupetre,N., Peoc'h,K., Foncin,J.F. and Destee,A. (1999) Prominent psychiatric features and early onset in an inherited prion disease with a new insertional mutation in the prion protein gene. *Brain*, **122**, 2375–2386.
4. Goldfarb,L.G., Brown,P., McCombie,W.R., Goldgaber,D., Swergold,G.D., Wills,P.R., Cervenakova,L., Baron,H., Gibbs,C.J. and Gajdusek,D.C. (1991) Transmissible familial Creutzfeldt-Jakob disease associated with five, seven and eight extra octapeptide coding repeats in the PRNP gene. *Proc. Natl Acad. Sci. USA*, **88**, 10926–10930.
5. Wopfner,F., Weidenhöfer,G., Schneider,R., von Brunn,A., Gilch,S., Schwarz,T.F., Werner,T. and Schätzl,H.M. (1999) Analysis of 27 mammalian and 9 avian PrPs reveals high conservation of flexible regions of the prion protein. *J. Mol. Biol.*, **289**, 1163–1178.
6. Liu,J.-J. and Lindquist,S. (1999) Oligopeptide-repeat expansions modulate protein-only inheritance in yeast. *Nature*, **400**, 573–576.
7. Chiesa,R., Piccardo,P., Ghetti,B. and Harris,D.A. (1998) Neurological illness in transgenic mice expressing a prion protein with an insertional mutation. *Neuron*, **21**, 1339–1351.
8. Chiesa,R., Drisaldi,B., Quaglio,E., Migheli,A., Piccardo,P., Ghetti,B. and Harris,D.A. (2000) Accumulation of protease-resistant prion protein (PrP) and apoptosis of cerebellar granule cells in transgenic mice expressing a PrP insertional mutation. *Proc. Natl Acad. Sci. USA*, **97**, 5574–5579.
9. Brown,D.R., Qin,K., Herms,J.W., Madlung,A., Manson,J., Strome,R., Fraser,P.E., Kruck,T., von Bohlen,A., Schulz-Schaeffer,W., Giese,A., Westaway,D. and Kretzschmar,H. (1997) The cellular prion protein binds copper in vivo. *Nature*, **390**, 684–687.
10. Waggoner,D.J., Drisaldi,B., Bartnikas,T.B., Casareno,R.L., Prohaska,J.R., Gitlin,J.D. and Harris,D.A. (2000) Brain copper content and cuproenzymes activity do not vary with prion protein expression level. *J. Biol. Chem.*, **275**, 7455–7458.
11. Lück,R., Steger,G. and Riesner,D. (1996) Thermodynamic prediction of conserved secondary structure: application to the RRE element of HIV, the tRNA-like element of CMV and the mRNA of prion protein. *J. Mol. Biol.*, **258**, 813–826.
12. Wills,P.R. and Hughes,A.J. (1990) Stem loops in HIV and prion protein mRNAs. *J. Acquir. Immune Defic. Syndr.*, **3**, 95–97.
13. Wills,P.R. (1992) Potential pseudoknots in the PrP-encoding mRNA. *J. Theor. Biol.*, **159**, 523–527.
14. Draper,D.E., Gluick,T.C. and Schlax,P.J. (1998) Pseudoknots, RNA folding and translational regulation. In Simons,R.W. and Grunberg-Manago,M. (eds), *RNA Structure and Function*. Cold Spring Harbor Laboratory Press, Plainview, NY, pp. 415–436.
15. Safar,J., Wille,H., Itri,V., Groth,D., Serban,H., Torchia,M., Cohen,F.E. and Prusiner,S.B. (1998) Eight prion strains have PrP(Sc) molecules with different conformations. *Nature Med.*, **4**, 1157–1165.
16. Le,S.H. and Maizel,J.V. (1989) A method for assessing the statistical significance of RNA folding. *J. Theor. Biol.*, **138**, 495–510.
17. Seffens,W. and Digby,D. (1999) mRNAs have greater negative folding free energies than shuffled or codon choice randomized sequences. *Nucleic Acids Res.*, **27**, 1578–1584.
18. Forsdyke,D.R. (1995) A stem-loop kissing model for the initiation of recombination and the origin of introns. *Mol. Biol. Evol.*, **12**, 949–958.
19. de Smit,M.H. and van Duin,J. (1990) Control of prokaryotic translational initiation by mRNA secondary structure. *Prog. Nucleic Acids Res.*, **38**, 1–35.
20. Love,H.D.,Jr, Allen-Nash,A., Zhao,Q. and Bannon,G.A. (1988) mRNA stability plays a major role in regulating the temperature-specific expression of a tetrahymena thermophila surface protein. *Mol. Cell. Biol.*, **8**, 427–432.
21. Gautheret,D., Major,F. and Cedergren,R. (1990) Pattern searching/alignment with RNA primary and secondary structures: an effective descriptor for tRNA. *Comp. Appl. Biosci.*, **6**, 325–331.
22. Altschul,S.F., Gish,W., Miller,W., Myers,E.W. and Lipman,D.J. (1990) Basic local alignment search tool. *J. Mol. Biol.*, **215**, 403–410.
23. Major,F., Turcotte,M., Gautheret,D., Lapalme,G., Fillion,E. and Cedergren,R. (1991) The combination of symbolic and numerical computation for three-dimensional modeling of RNA. *Science*, **253**, 1255–1260.
24. Rivas,E. and Eddy,S.R. (1999) A dynamic programming algorithm for RNA structure prediction including pseudoknots. *J. Mol. Biol.*, **285**, 2053–2068.
25. Franch,T., Petersen,M., Wagner,E.G.H., Jacobsen,J.P. and Gerder,K. (1999) Antisense RNA regulation in prokaryotes: rapid RNA/RNA interaction facilitated by a general U-turn loop structure. *J. Mol. Biol.*, **294**, 1115–1125.
26. Hermann,T. and Westhof,E. (1999) Non-watson-crick base pairs in RNA-protein recognition. *Chem. Biol.*, **6**, R335–R343.
27. Brooks,B.R., Bruccoleri,R.E., Olafson,B.D., States,D.J., Swaminathan,S. and Karplus,M. (1983) CHARMm: a program for macromolecular energy, minimization and dynamics calculations. *J. Comp. Chem.*, **4**, 187–217.
28. MacKerell,A.D.,Jr, Bashford,D., Bellott,M., Dunbrack,R.L.,Jr, Evanseck,J.D., Field,M.J., Fischer,S., Gao,J., Guo,H., Ha,S. *et al.* (1998) All-atom empirical potential for molecular modeling and dynamics studies of proteins. *J. Phys. Chem. B*, **102**, 3586–3616.
29. Davis,M.E., Madura,J.D., Luty,B.A. and McCammon,J.A. (1991) Electrostatics and diffusion of molecules in solution: simulations with the university of houston brownian dynamics program. *Comp. Phys. Commun.*, **62**, 187–197.
30. Sondheimer,N. and Lindquist,S. (2000) Rnq1: an epigenetic modifier of protein function in yeast. *Mol. Cell*, **5**, 163–172.
31. Simonic,T., Duga,S., Strumbo,B., Asselta,R., Ceciliani,F. and Ronchi,S. (2000) cDNA cloning of turtle prion protein. *FEBS Lett.*, **469**, 33–38.
32. Gutell,R.R., Cannone,J.J., Konings,D. and Gautheret,D. (2000) Predicting U-turns in ribosomal RNA with comparative sequence analysis. *J. Mol. Biol.*, **300**, 791–803.
33. Scheffer,U., Okamoto,T., Forrest,J.M.S., Rytik,P.G., Muller,W.E.G. and Schroder,H.C. (1995) Interaction of 68-kDa TAR RNA-binding protein and other cellular proteins with prion protein-RNA stem-loop. *J. Neurovirol.*, **1**, 391–398.
34. Shamoo,Y., Tam,A., Konigsberg,W.H. and Williams,K.R. (1993) Translational repression by the bacteriophage T4 gene 32 protein involves specific recognition of an RNA pseudoknot structure. *J. Mol. Biol.*, **232**, 89–104.
35. Thanaraj,T.A. and Argos,P. (1996) Protein secondary structural types are differentially coded on messenger RNA. *Protein Sci.*, **5**, 1973–1983.
36. Hedge,R.S., Mastrianni,J.A., Scott,M.R., DeFea,K.A., Tremblay,P., Torchia,M., DeArmond,S.J., Prusiner,S.B. and Lingappa,V.R. (1998) A transmembrane form of the prion protein in neurodegenerative disease. *Science*, **279**, 827–834.